Polyhedron 57 (2013) 94–104

Contents lists available at SciVerse ScienceDirect

Polyhedron

journal homepage: www.elsevier.com/locate/poly

Experimental and theoretical studies of a new donor–acceptor Re(I) complexes using nitropolypyridil ligand. Analysis of the NLO potential response

Luis Sanhueza [a], Mauricio Barrera [a], Irma Crivelli [b,*]

[a] Facultad de Quimica, Pontificia Universidad Católica de Chile, Casilla 306, Santiago, Chile
[b] Facultad de Ciencias Universidad de Chile, Las Palmeras 3425, Santiago, Chile

ARTICLE INFO

Article history:
Received 30 January 2013
Accepted 15 April 2013
Available online 19 April 2013

Keywords:
Orbital hardness
Transition metals
UV–Vis spectroscopy
Non linear optics
TD-DFT

ABSTRACT

A series of eight complexes with general structure $[ARe(CO)_3D]^+$, (A = NO_2phen, NO_2dppz; D = TBP, MOP, DMAP, PEPN) were synthesized and characterized by IR, NMR, UV–Vis spectroscopy and cyclic voltammetry. The donor and acceptor capacities, for the series of ligands employed, were measured in terms of two theoretical indexes, such as electrophilicity and orbital softness. It was found that, when the acceptor ligand is NO_2phen, an increase of the donor strength on the ligand causes a change in the first oxidation potential and slight change in the stretching frequencies of the NO_2 group, but not of the carbonyl group. This behavior is not observed when the acceptor ligand is NO_2dppz. The character of the absorption band (MLCT), ILCT, etc.), and the possibility of non linear optics activity of some of the complexes was analyzed. The calculated static hyperpolarizability, β_0, employing two different methods, indicates that the most promising complexes are those containing the PEPN ligand; the NLO behavior response is attributed to the enhancement of the non linear response of the PEPN ligand upon coordination to the $[Re(CO)_3D]^+$ fragment.

1. Introduction

Much attention has been devoted to study metal–carbonyl complexes in particular those of Re (I) with polypyridinic ligands. The aims of the research on this area are: (i) to know about the physicochemical properties of the fundamental and excited states and (ii) to apply this knowledge to the design of new materials with different potential applications and in relation with some processes (catalysis, LED, electron transfer process, etc.) [1,2]. As a consequence of the non linear optical properties (NLO) that are present in some of them, new potential applications emerge in the area of photonics [3]. For the specific case of inorganic complexes, the presence of a MLCT band appearing at low energy is associated with NLO response, since it should increase the degree of polarization occurring along the interaction of the ground state of the complex with a high intensity electromagnetic field. This conclusion is the result of the study of several metallic complexes. For the specific case of tricarbonyl polypyridinic complexes, it was found that their NLO response is determined by the presence of several factors. A similar conclusion was published by Le Bozec and Renouard [4] in their micro review of 2004.

For example, Wrighton et al. [5] used absorption and emission spectroscopy to get information on the relative importance of the $\pi\pi^*$, intra ligand charge transfer (ILCT) and metal to ligand charge transfer (MLCT) band, and they concluded that the energy of the MLCT band can be tuned modulating the electronic charge density on the Re(I) center; the correlation between the frequency of the emission (ν_{EM}) and the stretching vibration frequency of the CO ligand (ν_{ST}) gave support to this conclusion. Furthermore, if the ν_{ST} is taken as a measure of the electronic charge density on the Re(I) then a high ν_{ST} value implies less electronic charge density on Re(I) and, therefore, a decrease of the Re → CO back donation, yielding a more energetic MLCT [6]. A further study on carbonyl stretching frequencies employing Raman spectroscopy [7] enables the characterization of the excited states. As a consequence of these studies, the ν_{ST} of carbonyls becomes of increasing importance in the study of physicochemical properties of carbonyl complexes, either using stationary IR [8] and/or IR and Raman time resolved techniques, or else, as a complement on DFT and TDDFT calculations [9].

In 1987, Calabrese and Tam [10] correlated the NLO response of studied complexes with the presence of a low energy band with high extinction coefficient and a charge transfer (CT) character and π delocalization. In 1990 Cheng, Tam and Eaton [11] reported results related to M $(CO)_4$ (4-X(4-styrilpyridine) using the $-NO_2$ group as one of the X substituents. They found that a high acceptor

* Corresponding author. Tel.: +56 2 9787328; fax: +56 2 271 3888.
E-mail address: icrivell@uchile.cl (I. Crivelli).

0277-5387/$ - see front matter © 2013 Elsevier Ltd. All rights reserved.
http://dx.doi.org/10.1016/j.poly.2013.04.028

capacity lowers the energy of the MLCT, reduces the energy gap between the excited and ground state, and increases the value of the second-order hyperpolarizability parameter (β), a measure of the quadratic NLO response. As a consequence of these results, several works were devoted to elucidate the role played by ligands bearing acceptor/donor substituents. These findings can be summarized as follows: first, the type of substituent influences the crossover between the lowest $\pi\pi^*$ and the lowest MLCT [12]. Second, the nature of the emissive state depends on the identity of the substituents, evidencing once more the complexity of the photo-physics process in Re(I) complexes [13]. Third, it was found that strong electron-accepting substituted groups on styryl-bipyridine ligands diminish drastically dipolar moments and β values [14], even though the HOMO–LUMO gaps are of the same order of magnitude than those with strong donating groups. These results were not surprising for the authors, since the allowed electronic transitions, as in the case of strong accepting groups, are of higher energy and do not correspond to a HOMO–LUMO transition, which exhibits a negligible oscillator strength.

All the above mentioned studies represent one current strategy to obtain a NLO response in the presence of high electric fields and in the last years [15] several reviews were published confirming the increasing interest for this field.

The design and synthesis of new inorganic complexes containing donor and acceptor ends, linked through a metal center group or *via* a π backbone fragment, must generate non centrosymmetric dipoles structures with a MLCT band at low energy, which would increase the degree of polarization along the interaction between the ground state and the electromagnetic field.

In this context, it seems of fundamental interest to clarify the nature of the low energy band of theses complexes. In the particular case of the Re (I) carbonyl complexes, this is a major task since the high crystal field, the high extinction coefficient values of the high energy intra ligand (IL) band, and the relatively high energy charge transfer (CT) band, make them appear at the same wavelength range of the absorption spectra, sometimes, overlapped or masked. Otherwise, as it has been pointed out, the presence of ILCT and MLCT simultaneously can be detrimental for NLO activity when aligned with opposed vector directions [14,16].

In this paper we report the synthesis and physicochemical study of eight new Re(I) carbonyl complexes containing donor and acceptor groups. Experimental data are complemented with theoretical studies, which allow their comprehension as well as to analyze their comparative potential response as NLO material. Two different acceptor ligands (A) containing the $-NO_2$ substituents were used (A = NO_2 phen and NO_2dppz) and each of them was combined with four different donor groups (D = 4-terbutylpyridine, 4-methoxypyridine, 4-dimethylaminopyridine, p-[(N,N-dimethylamine)phenyl-o-styrene)]-pyridine).

2. Experimental

2.1. Materials

All the reagents used, the ligands 4-ter-butylpyridine and 4-methoxypyridine, the reagents 2,3-diamino-4-nitrobenzene, 4-methylpyridine, 4-dimethylaminobenzaldehyde and the solvents were purchased from Aldrich and used without further purification.

2.2. Physical measurements

Elemental Analyses were carried out on CE instruments *EA* 1108 model. UV–Vis absorbance measurements were made on a Shimadzu UV 3101PC spectrophotometer, while photoluminescence (PL) spectra were registered on Perkin Elmer L55 equipment.

Infrared Spectra: Infrared (IR) spectra for the desired compounds and reactants were recorded as KBr mulls on a Bruker Vector 22 FTIR spectrometer.

NMR: ^{1}H NMR spectra were recorded on a Bruker ACL 200 200 MHz spectrometer with TMS as reference or on a Bruker AVANCE 400 FT-NMR spectrometer.

Electrochemistry: Cyclic voltammetry was performed under nitrogen in saturated 0.1 M tetrabutylammonium hexafluorophosphate (TBAH) as supporting electrolyte in CH_3CN. A BAS model CV50w potentiostat was used in a standard three-electrode arrangement with a Pt or glassy platinum working electrode, a Pt gauze counter electrode, and a Ag/AgCl reference electrode.

2.3. Computational details

All the calculations were performed using the ADF 2009 package [17]. Geometrical optimizations were carried out with PW91 exchange functional in conjunction with TZP basis set for C,H,N,O and ZORA-TZ2P for Rhenium. This functional was chosen among others containing GGC, such as PBE, mPW91, BLYP and OLYP, since they turned out to be the best ones to reproduce crystallographic distances (Re–C, Re–N and C–O) of the parent complex $[Re(CO)_3(ACN)_2]^+$ [18] (Table S1). Structural data (atomic distances and bond angles) for the eight complexes are summarized on Tables S7 and S8.

The energy of the single occupied molecular orbital (E_{SOMO}) of ligands was calculated by optimizing the geometry of the corresponding single charged anion with PW91 and thereafter, running a single point energy calculation with the SAOP exchange correlation functional at the TZP level.

TDDFT studies were performed in the presence of solvent and employing several exchange–correlation functionals in order to choose which of them best reproduces the λ_{max} of the UV–Vis spectra of the PEPN ligand and the $[(NO_2phen)Re(CO)_3(PEPN)]^+$ complex in acetonitrile. Results (Table S2) show that the statistical averaged optimized exchange potential (SAOP) [19], an exchange potential model that was improved from the LB94 [20], in conjunction with SZ basis set for C, H, O, N and ZORA-TZP for Re, are the most suitable for spectroscopic studies of these compounds.

Reactivity indexes such as eletrophilicity (E^+), orbital hardness (η^+) and softness (σ^+), average polarizability (α_0) and static hyperpolarizability (β_{stat}) were calculated at the TZP levels and results compared with two other exchange–correlation functionals (LB94 and PBE [21]).

2.4. Theoretical background

With the aim to understand the effect caused by the acceptor–donor pairs of ligands on the observed physicochemical properties of the complexes, it is necessary to quantify the acceptor/donor strength of each ligand. From a theoretical point of view, the density functional theory (DFT) has provided two useful numerical descriptors for the present purpose, namely, the electrophilicity and the orbital hardness.

The electrophilicity index (E^+), derived by Parr and co-workers [22], is the measure of the acceptor power of a molecule and can be calculated by means of Eq. (1),

$$E^+ = \frac{\mu^2}{2\eta} \tag{1}$$

where μ is the chemical potential and η the absolute hardness. Both properties can be calculated in terms of the sum and difference between the ionization potential (I) and the electron affinity (EA).

However, when this data is not available, both indexes can be obtained theoretically employing the Koopman's theorem [23], which allows to replace I and A by the HOMO and LUMO eigenvalues. Otherwise, another possibility to assign values for μ and η can be found within the Kohn–Sham framework [24], where the chemical potential is identified with the frontier eigenvalue (ε_F), which in turn is the ionization potential. The electron affinity can be obtained from the single occupied molecular orbital eigenvalue (ε_S), hence giving,

$$\mu = \varepsilon_F \text{ and } \eta = \epsilon_F - \varepsilon_S \quad (2)$$

The second index of concern is the orbital hardness ($\eta^{\pm}$), which is a measure of the resistance of the frontier molecular orbital to release electronic charge. It was first conceived by Komorowski [25] and later calculated by Zuloaga [26] using the non-integer occupation number method:

$$\eta^{\pm} = \frac{\partial \varepsilon_F}{\partial n} = \frac{\varepsilon_F(1) \pm \varepsilon_F(dn)}{dn} \quad (3)$$

which measures the response of the change in the energy of the frontier orbital when the occupation number is subjected to a small change (dn). Accordingly, it follows that a good acceptor must exert a high resistance to deliver charge; therefore, its orbital hardness must be high, ensuring that the electronic charge will be retained. The complementary property of the orbital hardness is the orbital softness:

$$\sigma^{+} = \frac{1}{\eta^{+}} \quad (4)$$

This in turn measures how easily the frontier orbital can release its electronic charge. Therefore, it has also been related with polarizability [27], a measure of the deformation of the electronic cloud when subjected to an external electric field. According to this, an electron-donating molecule or a chemical group should possess a high orbital softness and must be highly polarizable. Indeed, for a molecule having no spherical symmetry, the polarizability would be characterized in terms of the average polarizability ($\overline{\alpha_0}$):

$$\overline{\alpha_0} = \frac{1}{3}(\alpha_X + \alpha_Y + \alpha_Z) \quad (5)$$

2.5. Synthesis

2.5.1. Ligands

The synthesis of 5-nitro-1,10-phenantroline (NO_2Phen), [28a] and 11-nitrodipyrido [3,2-a:3′,2′-c]phenazine (**NO_2Dppz**) were carried out as described in the literature [28b]. The corresponding elemental analysis and ^{1}H NMR spectra were in agreement with the published results. Also, p-[(N,N-dimethylamino)phenyl-o-hydroxyl)]-pyridine and p-[(N,N-dimethylamino)phenyl-o-styrene)]-pyridine (**PEPN**), were obtained according to procedures described in the literature [29]. The corresponding elemental analysis and ^{1}H NMR spectra were in agreement with the published results and the latter spectra were enough to corroborate the "trans" symmetry regarding to the "vinyl spacer" through the strong coupling (c.a. J = 16 Hz) of each proton (see ^{1}H NMR characterization). Fig. 1 shows the proton labels.

2.5.2. Complexes with acceptor group (precursor complexes)

fac-[(NO_2phen)Re(CO)$_3$Cl]. 200 mg (0.553 mmol) of [Re(CO)$_5$Cl] and 124 mg (0.553 mmol) of phen-NO_2 are dissolved in 40 mL of toluene. The mixture is heated to reflux for 2.5 h. During this period an orange solid is formed. Then, all the solvent is removed under vacuum. The solid is washed several times with diethyl ether and dried under vacuum. Yield: 70%. IR, KBr (cm^{-1}): ν_{C-O} = 2021, 1902, 1882 ν_{C-NO2} = 1518, 1341: $\nu_{C-H(arom)}$ = 3086, 3049. ^{1}H NMR ($CDCl_3$) δ (ppm), J(Hz): 9.57 (dd, 1H, Ha; Ja,b = 5.20, Ja,c = 1.38), 9.54 (dd, 1H, Ha′, Ja′,c′ = 1.37, Ja′,b′ = 5.11), 9.39 (dd, Hc, Jc,a = 1.35, Jc,b = 9.16), 8.99 (s, 1H, Hd′), 8.77 (dd, 1H, Hc′, Jc′,b′ = 9.12, Jc′,a′ = 1.35), 8.07(m, 2H, Hb, Hb', Jb,a = 5.10; Jb,c = 915).

fac-[(NO_2dppz)Re(CO)$_3$Cl]. 140 mg (0.387 mmol) of [Re(CO)$_5$Cl] and 0.126 mg (0.387 mmol) of ddpz-NO_2 are mixed in 25 mL of toluene. The mixture is heated to reflux for 2 h. During this period an orange solid is formed. Then, the solid is filtered under vacuum and washed with small portions of diethyl ether and dried under vacuum. Yield: 85%. IR, KBr (cm^{-1}): ν_{C-O} = 2026, 1918, 1880, ν_{C-NO2} = 1523, 1346, $\nu_{C-H(arom)}$ = 3074. ^{1}H NMR (DMSO-d$_6$) δ (ppm), J(Hz): 9.81 (dd, 2H, Hc, Hc′, Jc,a = 1.41; Jc,b = 8.26), 9.56 (dd, 2H, Ha, Ha′; Ja,b = 5.26; Ja,c = 1.35), **9.25** (s, 1H, Hd), 8.78 (d, 1H, He; Je′,d′ = 9,34), 8.67(d, 1H, Hd′; Jd′,e′ = 9.35), 8.28 (m, 2H, Hb, Hb′; Jb,a = 5.28, Jb,c = 8.01).

2.5.3. Complexes with donor (D) and acceptor (A) groups (A-Re(CO)$_3$-D complexes.)

General procedure: for a representative synthesis 150 mg of the precursor complex is mixed with three equivalents of donor ligand = 4-terbutylpyridine (**TBP**), 4-methoxypyridine (**MOP**), 4-dimethyaminopyridine (**DMAP**), N,N-dimethyl-4-[pyrydin-4-yl)ethenyl]aniline (**PEPN**) and three equivalents of $AgPF_6$ in 10 mL of dimethylformamide (DMF). The mixture is then heated to reflux for 2 h, protected from the exposure of light and under nitrogen atmosphere. Then, DMF is evaporated in a rotary evaporator. The remaining solid is dissolved in CH_2Cl_2, filtered through Celite and, after reducing the solution volume, precipitated by ethyl ether. The solid is filtered and washed with small portions of ethyl ether and dried under vacuum.

2.5.3.1. fac-[(NO_2phen)Re(CO)$_3$(TBP)]PF$_6$, ***1***. Yield: 72%. *Anal.* Calc. for [Re(I)$C_{24}H_{20}N_4O_5$]PF_6. (+0.2DMF) C, 37.39; H, 2.73; N, 7.44. Found: C, 37.49; H, 2.76; N, 7.40%. IR, KBr ($\nu_{CH3(arom)}$ = 3102; $\nu_{CH3(alif)}$ = 2968; ν_{C-O} = 2034, 1946, 1912; ν_{C-NO2} = 1519 1338,. ν_{PF6} = 841, 557, ^{1}H NMR ($(CD_3)_2CO$) δ (ppm), J(Hz): 10.07 (dd, 2H, Ha, Ha′, Ja,c = 1.23, Ja,b = 5.14), 9.49 (dd, 1H, Hc, Jc,a = 1.21, Jc,b = 8.73), 9.35 (dd, 1H, Hc′, Jc′,a′ = 1.26, Jc′,b′ = 8.71), 9.33 (s, 1H, Hd′), 8.52 (m, 2H, Hb, Hb′, Jb,a = 5.12, Jb,c = 8.74), 8.51 (dd, 2H, H1, H1′, J1,2 = 6.84), 7.36 (dd, 2H, H2, H2′, J2,1 = 6.85), 1,13 (s, 9H, $(-CH_3)_3$).

2.5.3.2. fac-[(NO_2phen)Re(CO)$_3$(MOP)]PF$_6$, ***2***. Yield: 66%. *Anal.* Calc. for [Re(I)$C_{21}H_{14}N_4O_6$]PF_6 (+0.4DMF): C, 34.24; H, 2.17; N, 7.91. Found: C, 34.28; H, 2.12; N, 7.85% IR, KBr (cm^{-1}) $\nu_{CH3(arom)}$ = 3097; $\nu_{CH3(alif)}$ = 2943: ν_{C-O} = 2033, 1919, ν_{C-NO2} = 1515, 1338,. ν_{PF6} = 844, 558, ^{1}H NMR ($(CD_3)_2CO$) δ (ppm), J(Hz): 10.12 (dd, 2H, Ha, Ha′, Ja,c = 1.25, Ja,b = 5.03), 9.57 (dd, 1H, Hc, Jc,a = 1.25, Jc,b = 8.75), 9.43 (dd, 1H, Hc′, Jc′,a′ = 1.21, Jc′,b′ = 8.32), 9.40 (s, 1H, Hd), 8.57 (m, 2H, Hb, Hb′, Jb,a = 5.16, Jb,c = 8.77) 8.44 (dd, 2H, H1,H1′, J1,2 = 7.03), 6.91 (dd, 2H, H2,H2′, J2,1 = 7.05), 3.88(s, 3H, O–CH_3).

2.5.3.3. fac-[(NO_2phen)Re(CO)$_3$(DMAP)]PF$_6$, ***3***. Yield: 72%. *Anal.* Calc. for [Re(I)$C_{22}H_{17}N_5O_5$]PF_6 (+0,2DMF): C, 34.93; H, 2.39; N, 9.36. Found: C, 34.98; H, 2.44; N, 9.32%. IR, KBr (cm^{-1}) $\nu_{CH3(arom)}$ = 3095; $\nu_{CH3(alif)}$ = 2927: ν_{C-O} = 2029, 1912, ν_{C-NO2} = 1520, 1396,. ν_{PF6} = 844, 557, ^{1}H NMR ($(CD_3)_2CO$) δ (ppm), J(Hz): 10.10 (dd, 2H, Ha, Ha′, Ja,c = 1.40, Ja,b = 5.23), 9.57 (dd, 1H, Hc; Jc,a = 1.38, Jc,b = 8.80), 9.43 (dd, 1H, Hc′, Jc′,a′ = 1.44, Jc′,b′ = 8.30), 9.42 (s, 1H, Hd), 8.57 (m, 2H, Hb, Hb′, Jb,a = 5.24, Jb,c = 8.79), 7.99 (dd, 2H, H1, H1′, J1,2 = 7.34), 6.45 (dd, 2H, H2, H2′, J2,1 = 7.35), 3.00(s, 6H, N–$(CH_3)_2$).

2.5.3.4. fac-[(NO_2phen)Re(CO)$_3$(PEPN)]PF$_6$, ***4***. Yield: 44%. *Anal.* Calc. for [Re(I)$C_{30}H_{23}N_5O_5$]PF_6 (+0,1toluene): C, 42.19; H, 2.75; N, 8.01. Found: C, 42.09; H, 2.93; N, 7.98%. IR, KBr (cm^{-1}) $\nu_{CH3(arom)}$ = 3091;

$\nu_{CH3(alif)}$ = 2919, 2810: ν_{C-O} = 2033, 1918, ν_{C-NO2} = 1523, 1334,. ν_{PF6} = 842, 557, ^{1}H NMR ($(CD_3)_2CO$) δ (ppm), J(Hz): 10.08 (dd, 2H, Ha, Ha′, Ja,c = 1.27, Ja,b = 5.19), 9.50 (dd, 1H, Hc, Jc,a = 1.23, Jc,b = 8.28), 9.35 (dd, Hc′, Jc′,a′ = 1.25, Jc′,b′ = 8.31), 9.32 (s,1H, Hd‘), 8.51(m, 2H, Hb, Hb′, Jb,a = 5.14, Jb,c = 8.81), 8.38 (dd, 2H, H1, H1′, J1,2 = 6.74), 7.39 (dd, 2H, H5, H5′, J5,6 = 8.79), 7.36 (dd, 2H, H2, H2‘, J2,1 = 6.74), 7.34 (d, 1H, H3, J3,4 = 16.20), 6.78 (d, 1H, H4, J4,3 = 16.22), 6.69 (dd, 2H, H6, H6′, J6,5 = 8.76), 2.98 (s, 6H, N–$(CH_3)_2$).

*2.5.3.5. fac-[(NO_2dppz)Re(CO)$_3$(TBP)]PF_6, **5**.* Yield: 73%. *Anal.* Calc. for [Re(I) $C_{30}H_{22}N_6O_5$]PF_6 (+0,4DMF): C, 41.32; H, 2.76; N, 9.88. Found: C, 41.33; H, 2.82; N, 9.78%. IR, KBr (cm^{-1}) $\nu_{CH3(arom)}$ = 3101; $\nu_{CH3(alif)}$ = 2966, 2908; ν_{C-O} = 2035, 1947, 1917; ν_{C-NO2} = 1525, 1348,. ν_{PF6} = 842, 558, ^{1}H NMR ($(CD_3)_2CO$) δ (ppm), J(Hz): 10.16 (dd, 2H, Hc,Hc′, Jc,a = 1.51, Jc,b = 8.29), 10.08 (dd, 2H, Ha, Ha′, Ja,b = 5.33, Ja,c = 1.42), 9.37 (d, 1H, Hd, Jd,e′ = 1.91), 8.93 (dd, 1H, He′, Je′,d′ = 9.36, Je′,d = 2,46), 8.81 (d, 1H, Hd′, Jd′,e′ = 9.36), 8.64 (dd, 2H, Hb, Hb′, Jb,a = 5.29, Jb,c = 8.32), 8.62 (dd, 2H, H1,H1′, J1,2 = 6.89), 7.48(dd, 2H, H2, H2′, J2,1 = 6.83), 1.21 (s, 9H, $(-CH_3)_3$).

*2.5.3.6. fac-[(NO_2dppz)Re(CO)$_3$(MOP)]PF_6, **6**.* Yield: 69%. *Anal.* Calc. for [Re(I)($C_{27}H_{16}N_6O_6$)]PF_6 (+0,4DMF): C, 38.45; H, 2.76; N, 10.18 Found: C, 38.42; H, 2.81; N, 10.15% IR, KBr (cm^{-1}) $\nu_{CH3(arom)}$ = 3103; $\nu_{CH3(alif)}$ = 2952, ν_{C-O} = 2033, 1940, 1916, ν_{C-NO2} = 1525, 1348,. ν_{PF6} = 842, 558, ^{1}H NMR ($(CD_3)_2CO$) δ (ppm), J(Hz): 10.16 (dd, 2H, Hc, Hc′, Jc,a = 1.78, Jc,b = 8.28), 10.08 (dd, 2H, Ha, Ha′, Ja,c = 1.77, Ja,b = 5.32), 9.37 (d, 1H, Hd, Jd,e′ = 1.84), 8.94 (dd, 1H, He′, Je′,d′ = 9.36, Je′,d = 1.76), 8,82 (d, 1H, Hd′, Jd′,e′ = 9.36), 8,63 (m, 2H, Hb, Hb′, Jb,a = 5.31, Jb,c = 8.28), 8.53 (dd, 2H, H1, H1′, J1,2 = 7.13), 6.95 (dd, 2H, H2, H2′; J2,1 = 7.14), 3.86(s, 3H, O–CH_3).

*2.5.3.7. fac-[(NO_2dppz)Re(CO) $_3$(DMAP)]PF_6, **7**.* Yield: 71%. *Anal.* Calc. for [Re(I)$C_{28}H_{19}N_7O_5$]PF_6 (+0,1DMF): C, 39.07; H, 2.34; N, 11.40. Found: C, 39.03; H, 2.39; N, 11.34%. IR, KBr (cm^{-1}) $\nu_{CH3(arom)}$ = 3098; $\nu_{CH3(alif)}$ = 2931: ν_{C-O} = 2030 1914, ν_{C-NO2} = 1528, 1348,. ν_{PF6} = 843, 557, ^{1}H NMR ($(CD_3)_2CO$) δ (ppm), J(Hz): 10.16 (dd, 2H, Hc, Hc′, Jc,a = 1.81, Jc,b = 8.30), 10.03 (dd, 2H, Ha, Ha′, Ja,c = 1.79, Ja,b = 5.29), 9.36 (d, 1H, Hd, Jd,e′ = 2.45), 8.93 (dd, 1H, He‘, Je′,d′ = 9.37, Je′,d = 2.47), 8.81 (d, 1H, Hd′, Jd′,e′ = 9.37), 8.61 (m, 2H, Hb, Hb′, Jb,a = 5.29, Jb,c = 8.26), 8.03 (dd, 2H, H1, H1′, J1,2 = 7.38), 6.51 (dd, 2H, H2, H2′, J2,1 = 7.37), 2.98 (s, 6H, N–$(CH_3)_2$).

*2.5.3.8. fac-[(NO_2dppz)Re(CO)$_3$(PEPN)]PF_6, **8**.* Yield: 40%. *Anal.* Calc. for [Re(I)$C_{36}H_{25}N_7O_5$]PF_6 (+0,2toluene) C, 45.59; H, 2.72; N,9.95. Found: C, 45.56; H, 2.83; N, 10.03%. IR, KBr (cm^{-1}) $\nu_{CH3(arom)}$ = 3096; $\nu_{CH3(alif)}$ = 2920: ν_{C-O} = 2033, ν_{C-NO2} = 1525, 1348,. ν_{PF6} = 843, 557, ^{1}H NMR ($(CD_3)_2CO$) δ (ppm), J(Hz): 10.16 (dd, 2H, Hc, Hc′, Jc,a = 1.44, Jc,b = 8.22), 10.11 (dd, 2H, Ha, Ha′, Ja,c = 1.51, Ja,b = 5.31), 9,36 (d, 1H, Hd, Jd,e′ = 2.40), 8,91 (dd, 1H, He′, Je′,d′ = 9.37, Je′,d = 2.48), 8.80 (d, 1H, Hd′, Jd′,e′ = 9.39), 8.64 (m, 2H, Hb, Hb′, Jb,a = 5.32, Jb,c = 8.22), 8.52 (dd, 2H, H1, H1′, J1,2 = 6.50), 7.46 (dd, 2H, H5, H5′, J5,6 = 8.78), 7.44 (dd, 2H, H2, H2′, J2,1 = 6.54), 7.40 (d, 1H, H3, J3,4 = 16.42), 6.82 (d, 1H, H4, J4,3 = 16.45), 6,72 (dd, 2H, H6, H6′, J6,5 = 8.79), 3.03 (s, 6H, N–$(CH_3)_2$.

3. Results and discusion

3.1. Synthesis and characterization

The general scheme of the synthesis of complexes is shown in Scheme 1.

The reaction occurs with high yield for most of the compounds, in agreement with the proposed formula. The IR spectra of the complexes exhibit the characteristic bands of the corresponding free ligands, showing the effect of coordination to the metal.

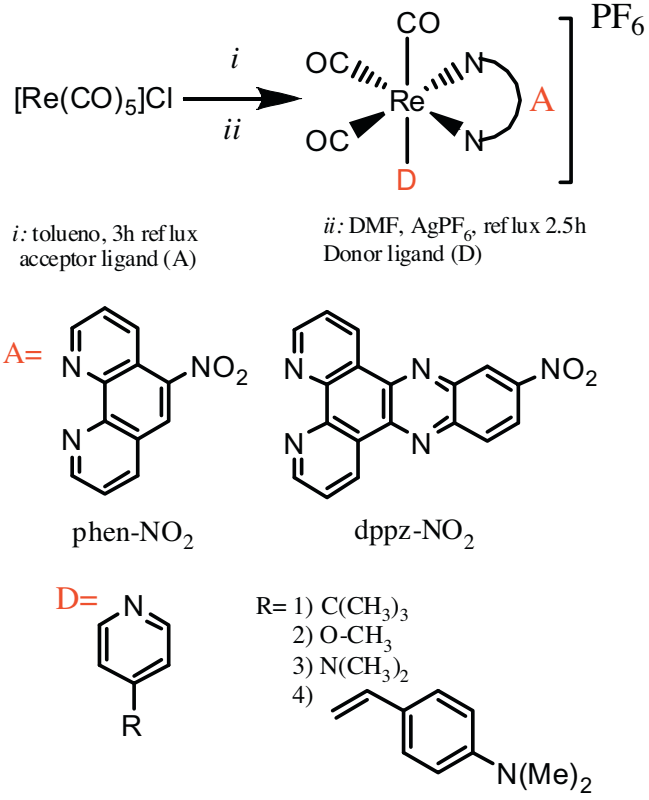

Scheme 1. Synthesis of $[(A)Re(CO)3D]^{+1}$ complexes.

All the metal-complexes display the IR frequencies characteristics of the -CO and –NO_2 groups in the range 2030–1910 and 1500–1390 cm^{-1}, respectively, as well the band for to the PF_6^- counter ion at 840 cm^{-1}.

For complexes **1** and **5** a band at 2968–3100 cm^{-1} was assigned to the methyl group on the tbpy substituent. Otherwise, complexes **2** and **6** display low intensity bands below 3000 cm^{-1} corresponding to the methoxy group. Complexes **3** and **7** show peaks at 2927 and 2931, respectively, assigned to the methyl group. Finally, complexes **4** and **8** show bands about 2920 due to the C–H aliphatic groups of the PEPN ligand.

The NMR spectra of the acceptor NO_2-phen and NO_2-dppz ligands (Table 1) show the corresponding proton signals, according to the loss of symmetry due to the NO_2 substituent. The qualitative comparison of the relative displacement of the Hb and Hb‘ signal positions of the free acceptor ligand and in the corresponding ([Re(I)$(CO)_3$ NO_2–L Cl]) precursor complexes, shows that the pres-

Table 1
^{1}H NMR results for Acceptor ligands and complexes [**1**–**8**].

	Ha	Ha′	Hb	Hb′	Hc	Hc′	Hd	Hd′	He′
NO_2phen	9.37	9.31	7.81		9.05	8.45	–	8.72	–
(**1**)	10.07		8.52		9.49	9.35	–	9.33	–
(**2**)	10.13		8.56		9.55	9.43	–	9.40	–
(**3**)	10.10		8.57		9.57	9.43	–	9.42	–
(**4**)	10.08		8.51		9.5	9.35	–	9.32	–
NO_2dppz	9.36		7.84		9.66		9.29	8.52	8.68
(**5**)	10.08		8.64		10.16		9.37	8.81	8.93
(**6**)	10.08		8.63		10.16		9.37	8.82	8.94
(**7**)	10.03		8.61		10.16		9.36	8.81	8.93
(**8**)	10.11		8.63		10.16		9.36	8.80	8.91

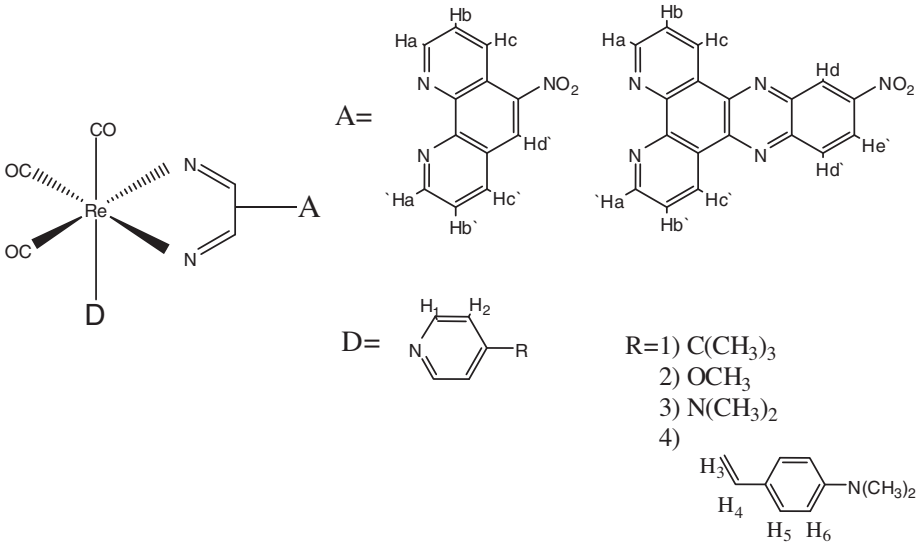

Fig. 1. Assignment of ^{1}H NMR signals.

ence of the Re(I)$(CO)_3$ fragment influences the electronic density distribution more than when the acceptor ligand is NO_2-dppz rather than NO_2-phen.

Most important is the analysis of NMR signals displacement in the $[ARe(I)(CO)_3D]^+$ complexes when the donor is changed. It can be noted that for the case of the complexes with the NO_2-phen li-

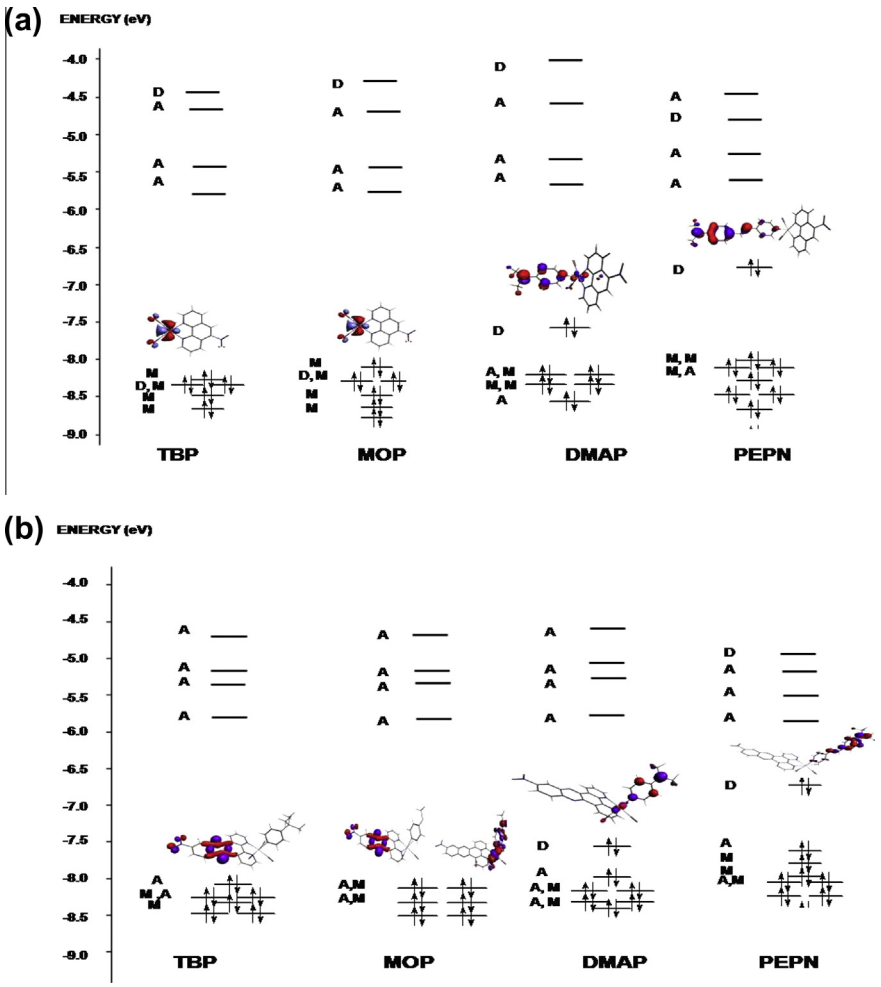

Fig. 2. Molecular Orbital Diagram for Complexes $[(A)Re(CO)_3D]^{+1}$, with D = TBP, MOP, DMAP, PEPN) and Acceptor ligands, (a) NO_2phen and (b) NO_2dppz also shown are isodensity plot of the HOMO for each complex.

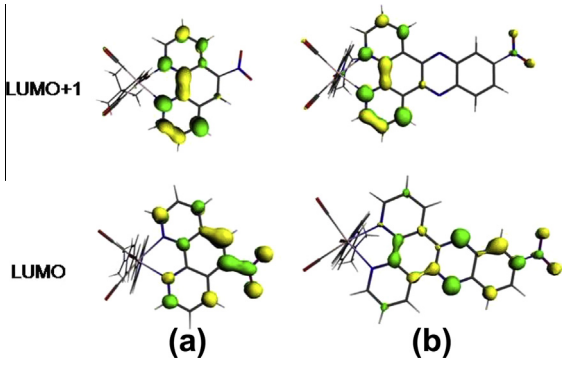

Fig. 3. Isodensity plots of LUMO and LUMO+1 for complexes containing (a) NO_2phen and (b) NO_2dppz acceptor ligands.

gand coordinated to Re(I), the change from the most to the less donor ligand has some effect on the ^{1}H NMR signal of NO_2-phen. Nevertheless, when the ligand is NO_2-dppz none of the ^{1}H NMR signals of this ligand changes at all. Thus, in the latter series of complexes, it seems that the enhancement of the capability of the donor ligand does not change the electron density on the dppz fragment of the acceptor ligand, as it does when the fragment is phen.

3.2. Molecular orbital analysis

Fig. 2 displays the molecular orbital diagram for (a) $[(NO_2phen)Re(CO)_3D]^{+1}$ and (b)$[(NO_2dppz)Re(CO)_3D]^{+1}$ complexes with different donor ligands (D).

The composition of each molecular orbital is displayed in Tables S3 and S4 (Supplementary material) in terms of molecular fragment. By comparing Fig. 2A and B it can be mentioned that the LUMO and LUMO+1 are always located on the acceptor ligand (A) (Fig. 3a and b), but with different electronic distribution. In the case of NO_2phen, the electronic density on this virtual level is distributed along the whole ligand while in the LUMO+1 it is located mainly on the bipyridine fragment. In the case of NO_2dppz, a different pattern is observed, since this ligand appears decomposed into two fragments: the first, on the nitro quinoxaline fragment of the LUMO and the second, on the bipyridine fragment of the LUMO+1 (Fig. 3b). For complexes bearing the NO_2dppz ligand (5–8), the greater localization of the charge on the LUMO would result in an increase of the transition dipole moment of a HOMO–LUMO excitation giving rise to different optical properties respect to those complexes containing the NO_2phen ligand. Another difference between NO_2phen and NO_2dppz complexes surges when comparing the change of the energy of the LUMO. For example, NO_2dppz complexes are more stabilized respect to the parent NO_2phen (−5.72 eV for **1** and −5.81 eV for **5**) and also for the latter a dependence of its energy upon the donor strength is found (−5.72 eV for TBP, complex **1** and −5.49 eV for PEPN, complex **4**). This influence is not observed on the NO_2dppz series (−5.81 eV for TBP, complex **5** and −5.82 eV for PEPN, complex **8**).

Focusing now on the analysis of the HOMO, Fig. 2a and b shows isodensity plots of this orbital for the eight complexes under study. As can be seen, when ligands with amino substituent (DMAP and PEPN) are employed, the HOMO of such complexes (**3**, **4**, **7** and **8**) is centered on this ligand. However, note that a different result is found indeed for those complexes bearing TBP and MOP ligands. For these cases, the HOMO is located on the metal, when the acceptor is NO_2phen (complexes **1** and **2**), and on the quinoxaline fragment when the ligand is NO_2dppz (complexes **5** and **6**). It is also noteworthy that for those complexes, the HOMO−1 possesses a metal character and lay 0.09 eV below for **5** and 0.04 eV for **6**. As a consequence of this, it follows that the energy of the frontier orbital is strongly influenced by the donor strength of the ligand since it rises from −8.27 eV for complex **1** or −8.06 eV for complex **4** to −6.71 eV for complex **4**(**8**). Moreover, it is noteworthy that for all complexes containing the metal center, the d-π orbitals of Rhenium appear combined with the π^+ molecular orbital from the carbonyls, hence giving rise to a back donation.

Table 2
Comparison of first and second reduction potentials (in Volts) of acceptor ligands with the E_{SOMO} energy (eV).

Acceptor	E_{SOMO}	$E_{½}$ (0/−I)	$E_{½}$ (−I/−II)
NO_2Phen	−3.06	−1.28	−2.06
NO_2Dppz	−4.10	−1.08	−1.56

3.3. Electrochemistry

Table 2 displays the first and second reduction potential for the acceptor free ligands, and the energy of the single occupied molecular orbital (SOMO). As was previously found for this type of polypyridinic ligand [30], the lowest reduction potential is found on the ligand with lower ε_{SOMO} and highest electrophilicity. In our case the ligand with these characteristics corresponds to the NO_2dppz ligand, which also shows the lowest reduction potential. These results imply that this NO_2dppz ligand is a better acceptor than NO_2phen. Indeed, it is noteworthy that although both ligands possess the same planar and aromatic structure, they differ on the pyrazine ring condensed to the phenantroline ligand. Presumably, this ring would be responsible for the enhancement of the electron-acceptor capacity of the ligand, which can also be observed on analyzing the second reduction potential, which is significantly higher on NO_2dppz (−1.56 V) than on NO_2Phen (−2.06 V), showing that the former ligand possess a higher electronic acceptance capacity than the latter.

Table 3 displays the oxidation potential of the metal center and the first reduction peak for the series of complexes under study. The Re(I)/Re(II) is an irreversible oxidation process and the values are independent of the direction of the scan. From the analysis of this table, three interesting features can be pointed out: (1) The electronic density around Re(I) shows low sensitivity to the donor ligand capacity but with a clear tendency to increase with the increase of the donor capacity. The apparent discrepancy of the values with DMAP and PEPN as substituents is explained since in these cases the oxidation of the metal center occurs after the oxidation of the amine group. (2) A low influence on the aromaticity of the acceptor ligand is observed. (3) The value of the first reduction potential is not influenced by the nature of the donor group and is only slightly affected by the nature of the acceptor ligand. (4) The coordination to the metal group produces a much greater change on the electronic density in NO_2phen than in NO_2dppz, independently of the π donor group, since the value of the first

Table 3
REDOX properties of the A-Re(CO)$_3$-D complexes.

Aceptor	Donor	$E_{½}$ (0/I)[a]	E_{ox} (I/II)[a]	$E_{½}$ (0/−I)[a]
NO_2Phen	TBP	–	1.56	−0.89
	MOP	–	1.55	−0.90
	DMAP	1.28	1.54	−0.91
	PEPN	0.44	1.52	−0.90
NO_2Dppz	TBP	–	1.54	−0.86
	MOP	–	1.48	−0.87
	DMAP	1.29	1.51	−0.86
	PEPN	0.45	1.50	−0.88

[a] In Volt.

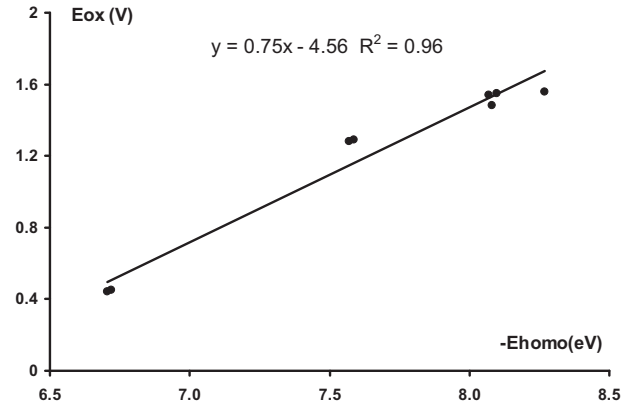

Fig. 4. Linear relationship between the first oxidation potential of the complexes and the energy of the corresponding highest occupied molecular orbital for the eight complexes under study.

reduction potential of both coordinated ligands differs only by 0.03 V, compared with the difference of 0.20 V when they are uncoordinated. The electrochemical experimental results for the complexes show consistency with the theoretical MO calculations. Fig. 4 shows the linear relationship, with correlation coefficient 0.96, between the first oxidation and the HOMO energy.

This relationship emerges from the Kohn–Sham theory, which states that the frontier eigenvalue is the ionization potential. However, since solvent effects are included in the present calculations, a correlation between the HOMO eigenvalue and the first oxidation potential is expected. This relationship opens the possibility to employ theoretical information to gain insight on the trend of electrochemical experimental results. In this sense, and looking at the experimental data in Table 3, it can be observed that an oxidation process occurs at 1.28 and 0.44 V for complexes with DMAP and PEPN ligands, respectively. These are irreversible processes and, in accordance with MO results from Fig. 1, this signal can be attributed to the oxidation of the amino group [31] Furthermore MO orbital calculations also establishes that the LUMO orbital is centered on the acceptor ligand, which can explain the independence of the first reduction potential respect to the donor ligand identity. An apparent discrepancy between theory and experiment is found for complexes bearing the NO_2dppz ligand and the acceptor TBP, for which, cyclic voltammetry measurements show that the first oxidation peak corresponds to the oxidation of the metal while the calculated HOMO is centered on the acceptor ligand. Nevertheless, it must be taken into account that the energy difference between the HOMO and the HOMO-1, which presents metal contributions, is within the range of accuracy of the calculations method.

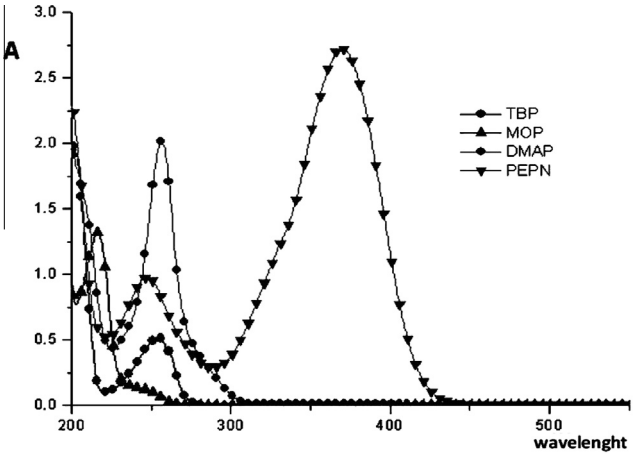

Fig. 5. Experimental absorption spectra of pyridine substituted ligands.

3.4. UV–Vis absorption spectra

- Donor ligands

Fig. 5 shows the experimental UV–Vis spectra of the four ligands under study. For the first three, TBP, MOP and DMAP, a characteristic π–π^* band appears between 250 and 270 nm.

For the case of PEPN a new absorption band with high extinction coefficient (21 700 M^{-1} cm^{-1}) is observed at 366 nm. With the aim to elucidate its composition a TDDFT calculation was performed.

Table 4 displays results for the three exchange–correlation functionals under consideration; the most accurate appear to be SAOP, followed by PBE. The increase of the basis set size causes a bathochromic shift of 54 nm on the calculated values while the inclusion of polarization functions does not improve the obtained values. In accordance to these results, the SAOP exchange–correlation functional, in conjunction with SZ basis set for C, H, O, N, should be the best choice for reproducing the experimental absorption spectra.

The transition density analysis shown in Fig. 6 for this ligand reveals that the electronic transition observed at 375 nm (a) corresponds mainly to a HOMO–LUMO excitation were the HOMO is centered on the 4-dimethylaminophenyl fragment of the molecule while the LUMO is on the 4-ethenyl pyridine fragment accordingly, it can be classified as an intramolecular charge transfer (ICT).

On the other hand, Fig 6(b) shows the transition density arising from the electronic transition occurring at 250 nm. The TDDFT results show that this transition involves a HOMO−2 to LUMO excitation, which is centered on the vinyl moiety and can be classified as $\pi \rightarrow \pi^*$.

- Acceptor ligands

The UV spectra of both acceptor ligands are displayed on Fig. 7. Both spectra show similar features: two bands located between 200 and 300 nm and a third, flat and broad, lying between 300 and 400 nm. In general, the λ_{max} of NO_2dppz ligand appears red shifted respect to NO_2phen. This is particularly observable in the third band, which reaches up to 390 nm in the former.

Table 4
Influence of the Exchange Correlation functional and the basis set on the TDDFT calculated λ_{max} of the PEPN ligand in acetonitrile.

	SZ	DZ	DZP
SAOP	377	431	434
LB94	403	452	456
PBE	389	444	445

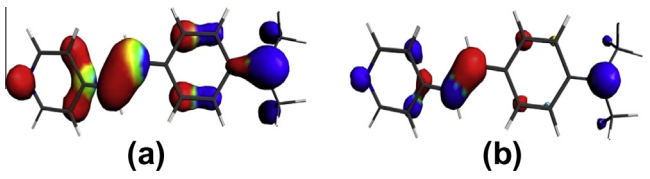

Fig. 6. Transition density corresponding to electronic transitions of the PEPN ligand at: (a) λ_{max} = 375 nm and, (b) λ_{max} = 250 nm (blue: starting density, red: ending density).

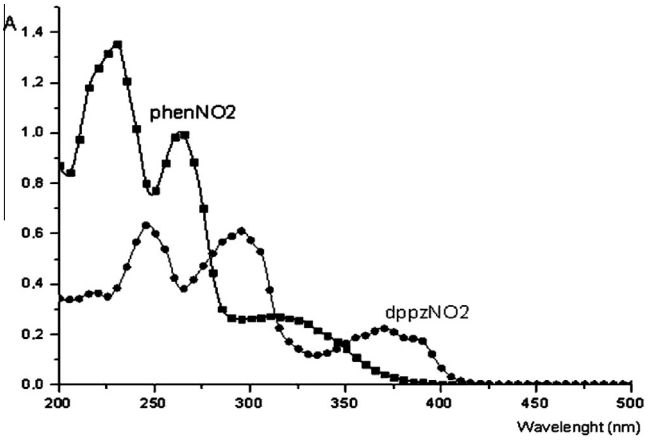

Fig. 7. Experimental absorption Spectra of NO_2phen and NO_2dppz.

- Complexes

The UV–Vis spectra for the NO_2phen and NO_2dppz series are displayed through Fig. 8a and b.

All the spectra show two main bands: one narrow and located between 200–300 nm with molar extinction coefficient between 20000 and 30000 M^{-1} cm^{-1} for TBP, MOP and PEPN but increased up to 50000 M^{-1} cm^{-1} when the donor is DMAP; this band can be attributed to a n, $\pi \rightarrow \pi^*$ electronic transition. The second band, which is broad and unstructured, appears as a shoulder in most complexes and is located between 300 and 500 nm, with a molar extinction coefficient around 5000–10000 M^{-1} cm^{-1} for TBP, MOP and DMAP donors. When the donor is PEPN the shoulder disappears giving rise to a well defined band with Gaussian shape and an increased molar extinction coefficient of 30000 M^{-1} cm^{-1}, with a maximum at 420 nm (Tables 4 and 5). Complexes with the dppz ligand exhibit a higher extinction molar coefficient compared to their similar complexes with NO_2Phen, with the exceptions of those with PEPN as donor ligand, where the extinction molar coefficient has a value of 30500 and 40000 M^{-1} cm^{-1} for both.

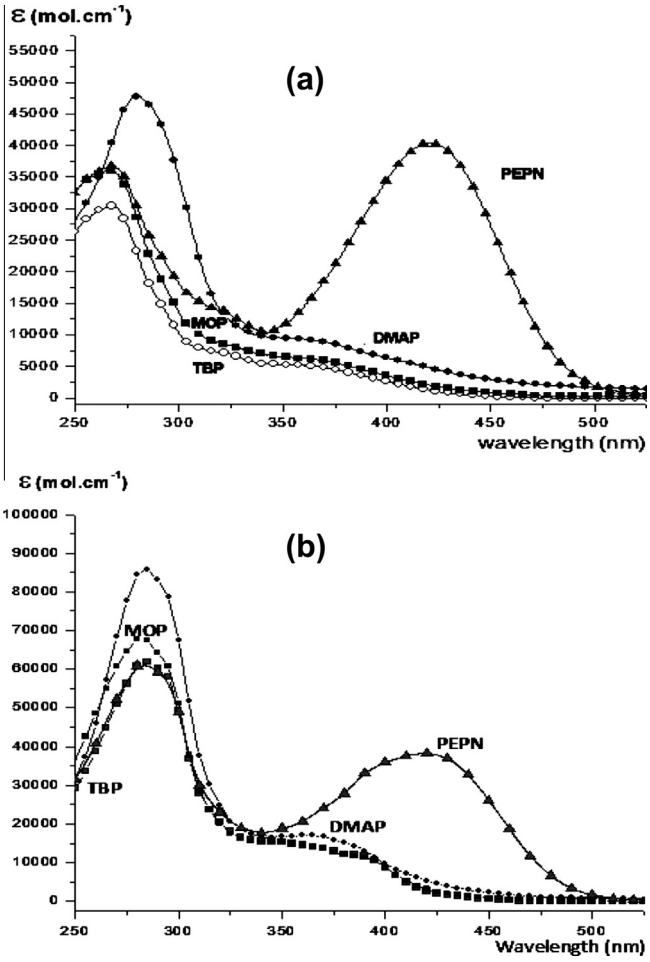

Fig. 8. Experimental Absorption Spectra of $[(A)Re(CO)_3D]^{+1}$ in acetonitrile as solvent(D = TBP, MOP.DMAP, PEPN) for (a) A = NO_2phen and (b) A = NO_2dppz.

As mentioned in the introduction, these low energy bands are of the most importance from the NLO point of view if they have a CT character since they should enhance the degree of polarization occurring along the interaction of the ground state of the complex with a high intensity electromagnetic field.

With the purpose to elucidate its composition, a transition density analysis (TDA) [31] was performed allowing the assignment of electronic transitions, in terms of molecular fragments, within the wavelength range where the absorption occurs.

Results obtained from this analysis (Tables S5.1–5.8) are summarized in column 4 of Tables 5 and 6 and enable the assignment shown in column 5, which are the dominant basic excitations along the absorption band. From the above data, a difference on the composition of the band is observed between those compounds containing the NO_2phen ligand and those with NO_2dppz, for all the donor ligands. For the case of PEPN, the intra ligand charge transfer character of the band is greater on the NO_2phen than in NO_2dppz complexes. This assignment is in accordance with previous studies using the resonance Raman technique [32]. Nevertheless, it is noteworthy the role of the $Re(CO)_3$ center, which operates as a Lewis acid, causing a red shift of the PEPN coordinated ligand respect to the free ligand. This bathochromic displacement on the absorption band of the free ligand is also found by the calculations reported in this work. However, it is important to mention that the increase on the molar extinction coefficient from 30000 to 40000 $M^{-1}cm^{-1}$, must be related to the presence of 36% of Ligand to Ligand excitations (LL).

3.5. Theoretical characterization of ligands and complexes

In order to gain more knowledge about the behavior of ligands and complexes and their potential suitability for NLO devices, quantification of their acceptor /donor strength was made. In general, it should be expected that compounds displaying high donor strength should possess an electronic cloud that is easily deformable, accompanied by a high tendency to release electronic charge. These two properties are representative of species that behave like good donors. According to Pearsońs theory [33] of acid and bases, this can be measured in terms of two reactivity indexes: the hardness (η) or its reciprocal property, the softness (σ) and the polarizability (α) parameters. Table 7 summarizes calculated values for

Table 5
Experimental wavelength maxima (λ_{max}), molar extinction coefficient (ε), composition and global assignment of the UV–Vis absorption band for $[(NO_2phen)Re(CO)_3(-D)]^+$ complexes.

D	λ_{max} (nm)	ε (M^{-1} cm^{-1})	% Contribution			Assignment
			MLCT	ILCT	LL[a]	
TBP	356	5222	99	0	1	MLCT
MOP	346	6654	91	1	8	MLCT
DMAP	350	9462	51	33	16	MLCT + LL
PEPN	420	30485	8	84	8	ILCT

[a] LL: ligand to ligand charge transfer.

Table 6
Experimental wavelength maxima (λ_{max}), molar extinction coefficient (ε), composition and global assignment of the UV–Vis absorption band for [$(NO_2dppz)Re(CO)_3$(D)]+ complexes.

D	λ_{max} (nm)	ε (M^{-1} cm^{-1})	% Contribution			Assignment
			MLCT	ILCT	LL[a]	
TBP	351	15255	69	28	3	MLCT + ILCT
MOP	350	14593	54	11	35	MLCT + LL
DMAP	366	13704	55	30	15	MLCT + ILCT
PEPN	419	40362	0	63	37	ILCT + LL

[a] LL: ligand to ligand charge transfer.

Table 7
Calculated orbital softness (σ^+), average polarizability (α_0) and dipole moment (P).

Donor	σ^+	α_0	P
TBP	0.156	114	3.1
MOP	0.159	80	3.4
DMAP	0.174	101	5.0
PEPN	0.240	257	7.6

the orbital softness (σ^+), average polarizability (α_0) and dipole moment (p) for the four donor ligands under study. All of the calculated values are independent of the basis set used at the TZP level, while the three exchange–correlation functionals employed exhibit the same tendencies in all of the four donors. The calculated local softness predicts an increase in the donor strength according to the tendency,

$$TBP < MOP < DMAP < PEPN$$

This reveals that PEPN is the best donor ligand and TBP the worse one. This trend is also found when the calculated dipole moments are compared.

These results suggest that, as the donor strength of the ligand increases also does the dipole moment; hence the molecule becomes more polarized. The average ligand polarizability follows the same tendency, with the exception of the TBP ligand, which evidences the effect of other variables.

On the other hand, since all of these donors are coordinated to Rhenium, it seems feasible to find a correlation between donor strength and the oxidation potential of the metallic center: a better donor should deliver more electronic density to the metal center, lowering its oxidation potential. In this sense, a linear correlation coefficient of 0.90 is found between $E^0(Re^{+1}/Re^{+2})$ and σ^+ for complexes bearing the NO_2phen. For the case of NO_2dppz complex the linear correlation is lost ($r = 0.23$). On the other hand, it seems noteworthy that all the complexes with NO_2dppz are more easily oxidized that those with NO_2phen. Both facts could evidence a different redistribution of the delivered electronic density.

Focusing now on the acceptor strength, strong acceptors should exhibit a high capacity to store charge together with a high resistance to deliver it. In this sense, the electrophilicity index can be employed to measure the acceptor power of a molecule in conjunction with the orbital hardness. From Table 8, it can be seen how the introduction of the nitro moiety on the phen and dppz ligands influences the orbital hardness, electrophilicity and polarizability. Calculated values show the same trends for all the three exchange–correlation functional. As expected, the nitro substituent increases the acceptor strength of the phenantroline ligand, since its electrophilicity index increases by 1.7 units, and becomes more polarizable with an increase of almost 13% in α_0.

Table 8
Calculated orbital hardness (η^+), electrophilicity index (E^+), and average polarizability (α_0) for the series of acceptor ligands.

Acceptor	η^+	E^+	α_0
Phen	4.5	5.7	161
Dppz	4.1	7.1	272
NO_2phen	4.7	7.4	184
NO_2dppz	4.0	8.6	305

A similar response is obtained for dppz, despite of the increase on its electrophilicity by 1.5 units; its polarizability increase by 12% is higher (272 au) when compared to phen (161). In both ligands the hardness is not significantly affected when the nitro substituent is added.

3.6. IR response

It seems interesting to examine how the change of the donor strength of ligands could affect experimental properties like the IR frequencies of end groups.

In principle, the increase of the donor strength, which correlates with the increase of the orbital softness, would give rise to an increase on the amount of electronic density delivered to the $[Re(CO)_3LNO_2]^+$ (L = phen, dppz) fragment. This extra charge would be delocalized within the fragment and stored by the most electron-withdrawing groups NO_2 and CO. If this process occurs, a correlation between the IR frequencies of these groups and the donor strength should be observed. Analysis of correlation coefficients (Table S6) confirm a slight correlation between the donor strength and the stretching frequencies of the NO_2 group (corr. coef. = 0.84) in complexes with phen ligand. On the other hand, for complexes bearing the dppz ligand, a correlation between the donor strength and vibrations frequency of the CO group (corr. coef. = −0.78) is observed. It must be considered that when the frequency values change, this change is small; the relevant is the observed different tendency in the two complexes series.

The results from IR and ^{1}H NMR spectroscopy and the metal oxidation potential value show for the NO_2phen series a shift of the ^{1}H NMR signals of the acceptor ligand and a change of the Re oxidation potential with a good correlation factor (Fig. 4, corr. coef. = 0.95). It appears that both properties are tuned by the type of donor ligand. In the case of the NO_2dppz series no such shift is observed and the corresponding correlation is poor. These results suggest the occurrence of ground state charge reorganization, when ligands with different electron-donating power are coordinated. This process seems to be influenced by the type of acceptor ligand.

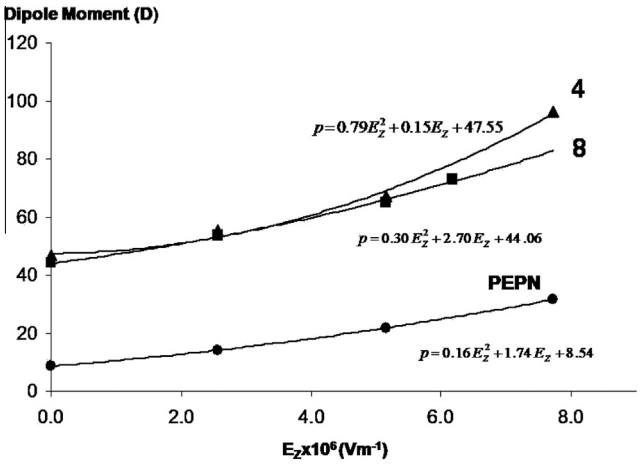

Fig. 9. Evolution of the dipole moment (in Debye) of the PEPN ligand and complexes **4** and **8** when they are subjected to an external electric field parallel to the z-axis.

Table 9
TDDFT data and calculated β_0 for ligand and complexes.

Complex	λ_{max} (nm)	E_{maz} (eV)	f_{osc}	p_{12} (D)	Δp (D)	$\beta_0^{TL} \times 10^{301}$ (esu)	$\beta_0 \times 10^{302}$		
							PBE	SAOP	LB94
PEPN (free)	377	3.29	0.67	7.2	12	58	73	68	80
[4]	444	2.79	0.72	8.2	12	127	136	132	*
[8]	444	2.79	1.23	10.8	9	162	145	148	*

[1] From Eq. (4).
[2] From ADF.
* No convergence.

3.7. The non linear optics potential response

Among the eight complexes under study, the most promising candidates to perform a study of their possible non linear optics quadratic activity would correspond to those two containing the PEPN ligand. In fact, although the other six complexes have a band with MLCT character, their energy is relatively high and the extinction coefficient is not so large, showing low values for the β_0 parameter (results not shown) Otherwise, the complexes containing the PEPN ligand present a strong absorption band in the visible region, which has ILCT character. This band, which is red shifted respect to the free ligand, indicates that the metal is acting as Lewis Acid upon the coordinated ligand, a behavior that has been pointed out to generate NLO activity [4].

In the present section, the quadratic non linear response of these complexes will be examined from a theoretical perspective by focusing our analysis on three features that gives rise to NLO response [34]: the response of the dipole upon an increase of the strength of an external electric field, the statistic hyperpolarizability and the composition of the lowest UV–Vis absorption band.

Fig. 9 shows for the three compounds the evolution of the dipole moment upon the increase of the strength of the external electric field applied, parallel to the z axis, which is aligned parallel to the molecular axis of the PEPN ligand and containing the nitrogen of the dimethylamine substituent and that of the pyridine.

The observed trend for the three molecules within the range of 0 to 8MVm^{-1} is best described by the second order degree equation: $p = p_0 + a\,E_Z + b\,E_Z^2$ and shows that coordination of the $[ARe(CO)_3]^+$ moiety to the donor ligand produces an increase of the dipole moment, which also boosts the value of the coefficient of the quadratic term from 0.16 to 0.79. By replacing the acceptor NO_2phen ligand of **4** by NO_2dppz of **8** a decrease of the curvature is also observed and the quadratic coefficient diminishes to 0.30.

This result must be examined with care since in this simple model it is supposed that all NLO response is attributed to the quadratic term of the dipole moment. A more sophisticated model would consider the calculation of the modulus of the β_{ijk} tensor as it is done on the ADF package [35] or from physicochemical model of two level(TL) [36].On calculating the modulus of the β_{ijk} tensor, the three exchange–correlation functional mentioned above were tested. However, the only reliable values were obtained for the PBE and SAOP functionals (Table 9), which shows that quadratic NLO activity of the free ligand is enhanced upon coordination to the metal. Comparatively, when the more electrophilic NO2dppz acceptor ligand is employed instead NO_2phen, a slightly high value on the nonlinear polarization can be observed.-Table 9 also shows results of calculations performed employing the two levels model (TL) [36] with data from TDDFT calculations; the purpose of the above is to understand what factors are responsible for the increase of the NLO response. According to this model, the static hyperpolarizability constant can be calculated with data obtained from the lowest absorption band, employing three physicochemical variables, according to Eq. (4).

$$\beta_0^{TL} = \frac{3\,p_{12}^2\,\Delta p}{E_{MAX}^2} \tag{6}$$

Here, p_{12} is the transition dipole moment, determined from the oscillator strength f_{osc} and E_{MAX} the energy where the molar extinction coefficient of the band is a maximum.

$$\|p_{12}\| = [f_{osc}/(1.08x10^{-8}\,E_{MAX})]^{1/2} \tag{7}$$

The change of the dipole moment, Δp, is usually determined through Stark spectroscopy, but in the present work it will be theoretically computed as the difference between the dipole moment of the ground state and that of the molecule on an excited state configuration resulting from a single Franck–Condon (adiabatic) excitation. For complex **4**, the responsible of the observed absorption band is mainly a HOMO–LUMO+3 excitation with ILCT character. For complex **8**, the main electronic transition occurs mainly from two excitations of the HOMO to LUMO+6 and to the LUMO+3, both with ILCT character. For both series of complexes, the change of the dipole moment is caused mainly by these excitations. In accordance with this assumption the β_0 value calculated through this model increases upon coordination to the metallic fragment due to the bathochromic shift of the band and to the fact that the increase of the transition dipole moment causes a greater oscillator strength. By comparing complexes **4** and **8**, two opposite side effects influencing the β_0 value are observed: the diminution of the change of the dipole moment (from 12D to 9D) and the increase of the oscillator strength (from 0.72 to 1.23). Due to the quadratic contribution of transition dipole moment on β_0, the final result will be an increase of the β_0 value. From the above results it can be concluded that the coordination of a metallic acceptor fragment to a donor organic ligand possessing an ILCT band at low energy increases its NLO behavior. The higher β_0 value for the complex **8**, when compared to complex **4**, can be attributed to the presence of *LL excitation*, which in the present work is obtained after a theoretical analysis, but it has also been reported in experimental works [37].

4. Summary and conclusions

Rhenium tricarbonyl complexes were designed to possess a push–pull structure, which is achieved by coordinating pairs of acceptor–donor ligands, taking in mind a potential NLO response. Experimental results were complemented with theoretical calculations in order to know which factors and molecular parameters determine such response and to predict qualitatively and comparatively the complexes with a better NLO response. The acceptor capacity is calculated in term of the electrophilicity index while for the donor strength we propose a new index based on the inverse of the orbital hardness. In this sense donor ligands can be classified with increasing donor strength according to:

TBP < MOP < DMAP < PEPN

On the other hand, a relationship is found between the donor strength and the redox potential, infrared frequencies and NMR signals shift, suggesting that for these complexes, a ground state

charge reorganization influenced by the type of acceptor ligand occurs, when ligands with different electron-donating power are coordinated,

A theoretical analysis using TD-DFT was performed on the spectroscopic data in order to disclose the nature of the lowest absorption band. The NLO response is also quantified by calculating the first static hyperpolarizability with two independent methods; a comparative analysis of the parameters that influence the β_0 value allows us the comprehensions of their values. When the donor ligand is the PEPN, the NLO response is related to an ILCT transition. The presence of an additional *Ligand to Ligand* transition in the complex containing NO_2dppz as acceptor ligand appears as an important contribution to enhance the NLO response.

Acknowledgement

The authors thank Fondecyt of Chile (Project Nos. 1070799 and 1110991).

Appendix A. Supplementary data

Supplementary data associated with this article can be found, in the online version, at http://dx.doi.org/10.1016/j.poly.2013.04.028.

References

[1] F. Barigelleti, I. Flamigni, Chem. Soc. Rev. 2 (2000) 1.
[2] N. Katz, J. Phys. Chem. 98 (1994) 8959.
[3] L. Ledoux, I. Zyss, in: I. Khoo, F. Simoni, C. Umeton (Eds.), Molecular Non Linear Optics: Fundamentals and Applications in Novel Optical Materials and Applications, Wiley, New York, 1997, p. 1 (Chapter 1).
[4] H. Le Bozec, T. Renouard, Eur. J. Chem. 80 (2000) 229.
[5] M. Wrighton, D. Morse, J. Organomet. Chem. 97 (1975) 405.
[6] S. Fredericks, J. Luong, M. Wrighton, J. Am. Chem. Soc. 101 (1979) 7415.
[7] W. Smothers, M. Wrighton, J. Am. Chem. Soc. 105 (1983) 106.
[8] L. Worl, R. Duessing, P. Cheng, L. Della Cianna, T. Meyer, J. Chem. Soc., Dalton Trans. 84 (1991) 849.
[9] (a) D. Dattelbaum, K. Omberg, J. Schoonover, R. Mertin, T. Meyer, Inorg. Chem. 41 (2002) 6071;
(b) D. Cleland, G. Irwing, W. Pawell, D. Officer, K. Gordon, Chem. Eur. J. 15 (2009) 3682.
[10] J. Calabrese, W. Tam, Chem. Phys. Lett. 133 (1987) 244.
[11] L. Cheng, W. Tam, Organometallics 9 (1990) 2856.
[12] R. López, B. Loeb, D. Striplin, M. Devenney, K. Omberg, T. Meyer, J. Chil. Chem. Soc. 49 (2004) 149.
[13] M. Kuimova, X. Zhong, P. Sun, P. Matousek, D. Grills, A. Parker, M. Towrie, M. George, Photochem. Photobiol. Sci. 6 (2007) 1158.
[14] A. Baccouche, B. Peigne, F. Ibersiene, D. Hammoutiene, A. Boutarfaia, A. Boucekkine, C. Feuvrie, O. Maurie, I. Ledoux, H. Le Bozec, J. Phys. Chem. 114 (2010) 5429.
[15] (a) E. Cariati, M. Pizzotti, D. Roberto, F. Tessore, R. Ugo, Coord. Chem. Rev. 250 (2006) 1210;
(b) B.J. Coe, Acc. Chem. Res. 39 (2006) 383;
(c) J.P. Morrall, G.T. Dalton, M.G. Humphrey, M. Samoc, Adv. Organomet. Chem. 55 (2007) 61;
(d) S. Di Bella, C. Dragonetti, M. Pizzotti, D. Roberto, F. Tessore, R. Ugo, in: H. Le Bozec, V. Guerchais (Eds.), Topics in Organometallic Chemistry 28. Molecular Organometallic Materials for Optics, vol. 28, Springer, 2010, p. 1.
[16] F. Vance, J. Hupp, J. Am. Chem. Soc. 121 (1999) 4047.
[17] G. Velde, F. Bickelhaupt, S. Van Gisbergen, C. Fonseca Guerra, E. Baerends, J. Snijders, T. Ziegler, J. Comput. Chem. 22 (2002) 931.
[18] Y. Lillian, E. Chan, E. Isaacs, A. Graham, Can. J. Chem. 55 (1977) 111.
[19] O. Gritsenko, Chem. Phys. Lett. 302 (1999) 199.
[20] R. Van Leeuwen, E. Baerends, Phys. Rev. A 49 (1994) 2421.
[21] J. Perdew, K. Burke, Phys. Rev. Lett. 77 (1996) 3865.
[22] R. Parr, L. Szentpaly, S. Liu, J. Am. Chem. Soc. 121 (1999) 1922.
[23] R. Parr, R. Pearson, J. Am. Chem. Soc. 105 (1983) 7512.
[24] W. Kohn, L. Sham, Phys. Rev. A 140 (1965) 1133.
[25] L. Komorowski, Chem. Phys. Lett. 134 (1997) 516.
[26] C. Goycolea, M. Barrera, F. Zuloaga, Int. J. Quantum Chem. 54 (1989) 123.
[27] M. Barrera, Int. J. Quantum. Chem. 111 (2011) 3097.
[28] (a) K. Binnemans, P. Lenaerts, K. Driesen, C. Gorller-Walrand, J. Coord. Chem. 54 (2001) 323;
(b) A. Arancibia, J. Concepcion, N. Daire, C. Leiva, A.M. Leiva, B. Loeb, R. Del Rio, R. Diaz, A. Francois, M. Saldivia, J. Coord. Chem. 54 (2001) 323.
[29] U. Hess, D. Huhn, J. Prakt. Chem. 325 (1983) 301.
[30] E. Norambuena, C. Olea-Azar, A. Delgadillo, M. Barrera, B. Loeb, Chem. Phys. 359 (2009) 92.
[31] F. Fajardo, M. Barrera, R. Vargas, I. Crivelli, B. Loeb, Inorg. Chem. 50 (2011) 5910.
[32] M. Waterland, K. Gordon, J. McGarvey, P. Jayaweera, J. Chem. Soc., Dalton Trans. 22 (1998) 609.
[33] R. Pearson, J. Am. Chem. Soc. 85 (1963) 3533.
[34] O. Maury, H. Le Bozec, in: B. Bruce, D. Ohare, R. Walton (Eds.), Metal-Based Quadratic Nonlinear Optics Materials on Molecular Material, John Wiley& sons, New York, 2009 (Chapter 1).
[35] S. Van Gisbergen, S. Snijders, E. Baerends, J. Chem. Phys. 109 (1998) 10644.
[36] J. Zyss, I. Ledoux, Chem. Rev. 94 (1994) 77.
[37] (a) C. Dragonetti, S. Righetto, D. Roberto, R. Ugo, A. Valore, S. Fantacci, A. Sgamellotti, F. De Angelis, Chem. Commun. 22 (2007) 4116;
(b) C.T. Chen, S.Y. Liao, K.J. Lin, L.L. Lai, Adv. Mater. 10 (1998) 334;
(c) D. Espa, L. Pilia, L. Marchiò, M. Laura Mercuri, A. Serpe, A. Barsella, A. Fort, S.J. Dalgleish, N. Robertson, P. Deplano Coord, Chem. Rev. 254 (2010) 1434.